Jurnal
Teknologi

Full Paper

FINITE ELEMENT ANALYSIS OF T-SECTION RC BEAMS STRENGTHENED BY WIRE ROPE IN THE NEGATIVE MOMENT REGION WITH AN ADDITION OF STEEL REBAR AT THE COMPRESSION BLOCK

Yanuar Haryanto[a,b*], Hsuan-Teh Hu[b], Han Ay Lie[c], Anggun Tri Atmajayanti[b,d], Dimas Langga Chandra Galuh[e], Banu Ardi Hidayat[b]

[a]Department of Civil Engineering, Faculty of Engineering, Jenderal Soedirman University, Purwokerto, Indonesia
[b]Department of Civil Engineering, College of Engineering, National Cheng Kung University, Tainan, Taiwan
[c]Department of Civil Engineering, Faculty of Engineering, Diponegoro University, Semarang, Indonesia
[d]Department of Civil Engineering, Faculty of Engineering, Atma Jaya Yogyakarta University, Yogyakarta, Indonesia
[e]Department of Civil Engineering, Faculty of Engineering, Sarjanawiyata Tamansiswa University, Yogyakarta, Indonesia

Article history
Received
15 July 2018
Received in revised form
29 April 2019
Accepted
2 May 2019
Published online
25 June 2019

*Corresponding author
yanuar.haryanto@unsoed.ac.id

Graphical abstract

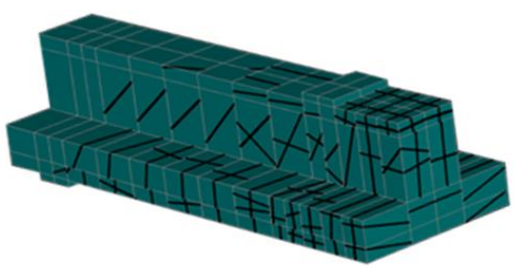

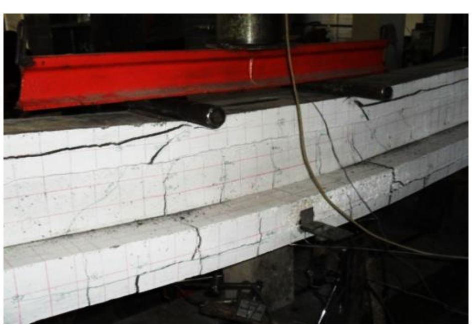

Abstract

A building whose functions are converted in which their volumes are improved, for example, a four-story building transformed into a five-story building, resulting in a dead load improvement of its structural self-weight, obviously requires strengthening in order to avoid the possibility of structural failures. This paper focuses on a nonlinear finite element analysis conducted using the ATENA program on T-section reinforced concrete beams strengthened in the negative moment region with wire ropes and an addition of steel rebars at the compression block. The results are then compared with the results of the previously conducted experiments. The specimen models consist of control beams (BK), strengthened beams with wire ropes at the tension block (BP1), and strengthened beams with wire ropes at the tension block and steel rebars at the compression block (BP2). The results show that the ratios of the load-carrying capacity against those of the experimental results are 1.25, 1.23, and 0.89 respectively for BK, BP1 and BP2. The effective stiffness ratios to those of the experimental results are 1.45, 1.15, and 1.86, while the ductility index ratios against the experimental results are 1.11, 0.63, and 1.01 respectively for BK, BP1, and BP2. The crack patterns of the nonlinear finite element analytical results revealed that all specimen models experience flexural failure.

Keywords: Finite element analysis, ATENA, reinforced concrete beam, strengthening, wire rope

1.0 INTRODUCTION

In the recent development era, many construction works have utilized reinforced concrete materials as their main structure, including for building. For their redevelopment to meet new needs, many buildings have been converted or their volumes have been improved to create new buildings. These functional changes and increased volumes require these structures to be reviewed due to the additional load capacity, which is beyond the previously designed load and may result in catastrophic structural failures or collapses, such as the case in South Korea of the Sampoong Department Store which was built in 1987–1989. Buildings which had previously functioned as a four-story office block were converted into a five-story department store. On 29 June 1995, Sampoong Department Store, the icon of the developing city of Seoul, collapsed in 20 seconds with 1,500 people inside. The collapse is the largest peacetime disaster in South Korean history – 502 people died, 6 missing, and 937 sustained injuries [1]. On the other hand, some elements of the structures may also have been weakened due to natural disaster that humans must be aware of its effect, just like earthquake [2-5].

Various experimental studies have focused on strengthening, especially, the reinforced concrete beam elements, in some cases utilizing wire ropes. Raoof and Davies [6] argued that wire ropes have greater flexibility, which accounts for their utilization for pulley traction elements in the mining field. The potential of wire rope for reinforced concrete has been examined [7] based on their other advantages, in the form of their high tensile strength. Kim *et al*. [8], who examined rectangular section reinforced concrete beams with shear strengthening utilizing wire ropes, stated that the diagonal type of strengthening may generate higher shear capacity than vertical strengthening. In fact, the greater the initial pre-stress force, the greater the shear capacity generated. A further study was conducted by Yang *et al*. [9] on a T-section beam strengthened with wire ropes, and they concluded that the closed type of strengthening is more effective than open strengthening in improving the capacity and ductility.

In Indonesia, an experimental study of the utilization of wire rope as a strengthening material for reinforced concrete beam elements was first conducted by Haryanto [10], and resulted in a flexural strength improvement of T-section reinforced concrete beams in the negative moment region with a ratio of 2.03. Further research was carried out by Atmajayanti *et al*. [11] which showed that the flexural strength improvement in the positive moment region has a ratio of 1.86. However, both argue that the resulting flexural strength improvement is generated after the higher cracks are developing and then propagating. Optimization was performed by Haryanto *et al*. [12] by applying an initial pre-stress force on the strengthening by utilizing two bonded wire ropes, which resulted in an initial pre-stress force of 20%, which provided a higher flexural strength improvement with a ratio of 1.91. Another method is to add steel rebars on the compression block for the T-section reinforced concrete beams strengthened with wire ropes in the negative moment region, which results in flexural strength improvement with a ratio of 2.93 [13, 14]. A current research on the wire rope performance as the external strengthening of reinforced concrete beams with different end-anchor types conducted by Haryanto *et al*. [15] who concluded that the ratios of end-anchor type 1 to end-anchor type 2 were close to 1 for all the parameters studied, which means that both types of end-anchor make an equally good contribution to the performance of wire rope.

From these experimental studies, it is seen that the results are precise but time-consuming and costly. The other current popular alternative is a finite element analysis. It utilises a program to validate the results of experimental studies [16]. Even though the outcomes of finite element analysis are only in the form of a theoretical approach, by understanding the working processes and through the use of accurate data, behaviors approaching the actual structural conditions may be obtained [17]. The finite element analysis has been employed successfully to investigate the influences of a series of parameters on the structural behavior of concrete structures [18]. One finite-element analysis computer program is ATENA [19]. Researches focused on the finite element analysis by utilizing ATENA have been conducted by Pangestuti and Effendi [20], Sukarno *et al*. [21], Setyawan [22], Jati [23], Haryanto *et al*. [24, 25], and Jirawattanasomkul *et al*. [26]. This paper studies finite element analysis by utilizing ATENA on T-section reinforced concrete beams strengthened in the negative moment region by wire ropes and the addition of steel rebars on the compression block, and then comparing the results with those of the experiments previously conducted [10, 12-14].

2.0 METHODOLOGY

2.1 Constitutive Models

Concrete is a heterogeneous material that is highly nonlinear. The constitutive basic models of concrete in ATENA use the concept of smeared cracking and the fracture mechanics approach. The stress reaction that takes place is based on the fracture concept of the uniaxial stress–strain law, which explains that the concrete fracture is due to monotonic loading, as shown in Figure 1. The peak stress at uniaxial behavior, $f_t'^{ef}$ and $f_c'^{ef}$, is determined based on the biaxial failure surface shown in Figure 2, according to the results of the study conducted by Kupfer *et al*. [27]. A simulated crack model is used to determine the concrete tension behavior based on the crack-opening law and fractural energy which is combined with the crack band.

In the ATENA program, the crack-opening law shown in Figure 3 uses an exponential function based on the study conducted by Hordijk [28]. For the condition of compression after peak stress, a simulated compression model is used as a basic assumption, adopted from the study conducted by Van Mier [29]. It is shown in Figure 4 that the tension failure is localized in the plane perpendicular to the principal stress direction. The two crack models in the ATENA program consist of fixed and rotated cracks. In the fixed crack (Figure 5), the crack direction is identical to the principal strain direction and changes due to directional changes of the strain. Meanwhile, the steel reinforcement constitutive model is based on bilinear and multilinear laws as shown in Figure 6.

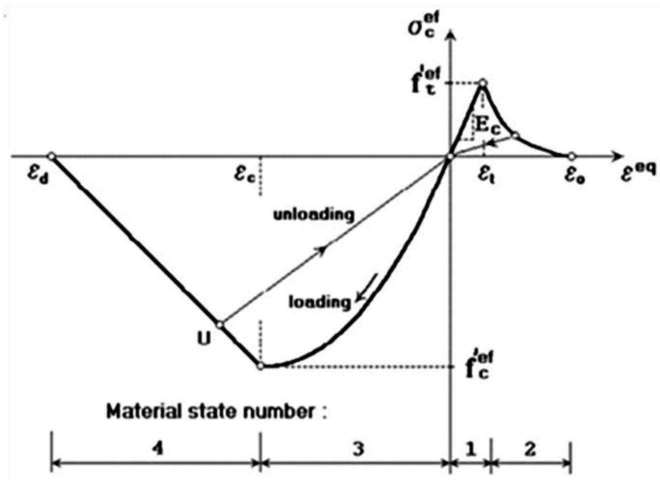

Figure 1 Uniaxial stress–strain law for concrete [15]

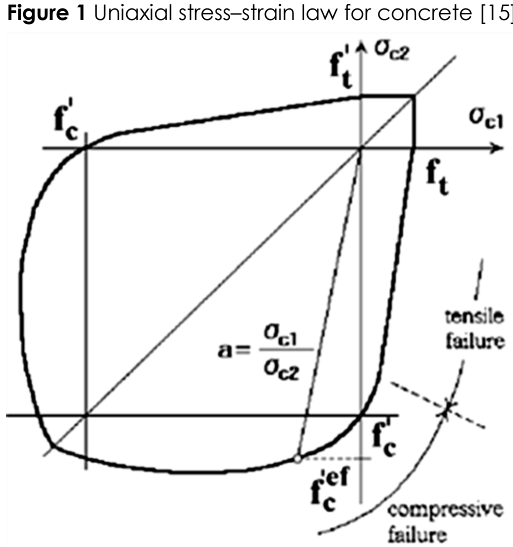

Figure 2 Biaxial failure function for concrete [15]

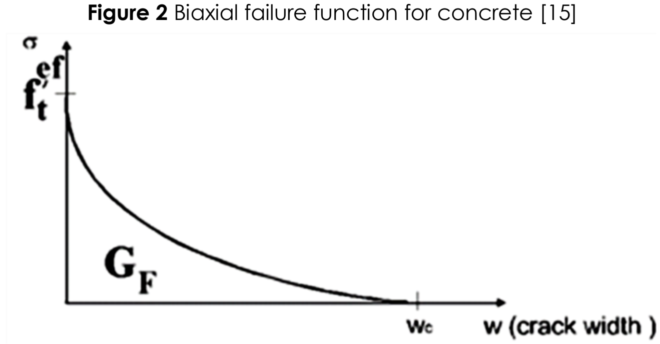

Figure 3 Exponential crack opening law [15]

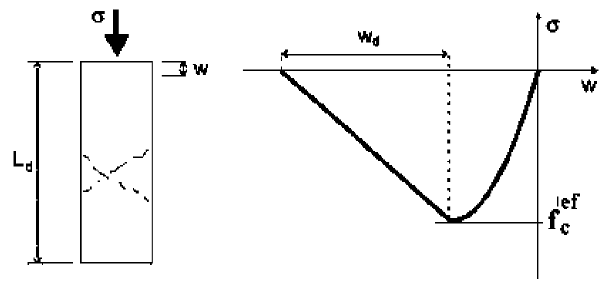

Figure 4 Softening displacement law in compression [15]

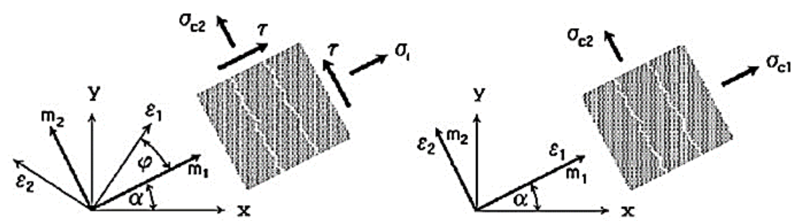

Figure 5 Fixed crack and rotated crack model [15]

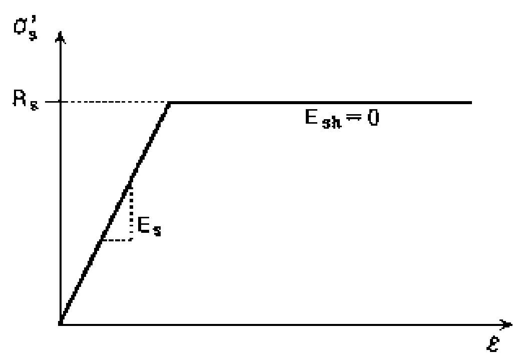

(a)

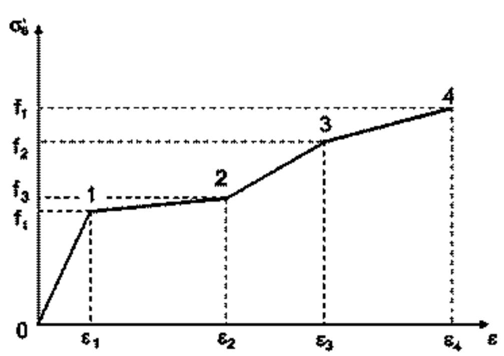

(b)

Figure 6 Stress–strain law for steel reinforcement: (a) bilinear stress–strain law; (b) multilinear stress–strain law

2.2 Specimen Model

The specimen model analyzed is in the form of T-section reinforced concrete beams with a span of 2.4 m, consisting of a control beam (BK), a beam without strengthening, strengthened beam type 1 (BP1) which has the strengthening of 4 wire ropes at the tension block bonded with mortar, and strengthened beam type 2 (BP2), which is strengthened with 4 wire ropes at the tension block and 2 steel rebars at the compression block in which both being bonded with mortar. The wire rope consists of six typical helical strands laid over a central core containing smaller independent wire ropes (IWRC), as shown in Figure 7, which is used as strengthening material of the negative moment region. Meanwhile, in the compression block, plain steel rebars are added. The details and the section of specimen models are presented in Table 1 and Figure 8.

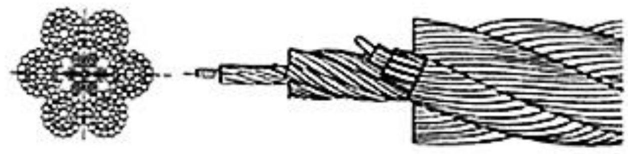

Figure 7 An independent wire rope core (IWRC) [2, 30]

Table 1 Details of specimen models

Codes	L (mm)	bf (mm)	tf (mm)	bw (mm)	Longitudinal reinforcement		Stirrup		Strengthening	
					Tensile	Compressive	Edge of span	Center of span	Wire rope	Steel rebar
BP	2400	400	75	150	3D13	2P8	P8-40	P8-100	-	-
BP1	2400	400	115	150	3D13	2P8	P8-40	P8-100	4D10	-
BP2	2400	400	115	150	3D13	2P8	P8-40	P8-100	4D10	2P8

D : Deform
P : Plain

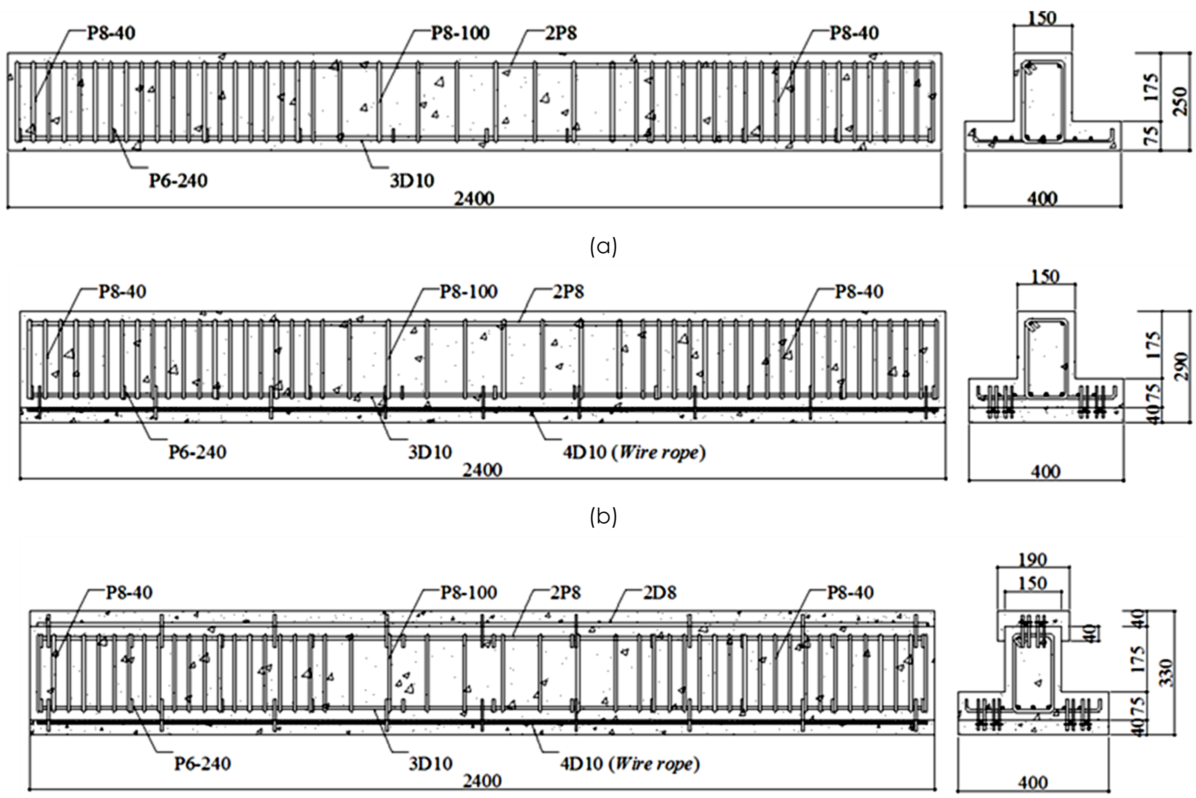

(a)

(b)

(c)

Figure 8 Section of specimen models: (a) control beam (BK); (b) strengthened beam type 1 (BP1); (c) strengthened beam type 2 (BP2)

All materials assumed to have a perfect bond. As the beams were symmetrical, the modeling could be conducted for half of a beam, as shown in Figure 9 for the BP2 specimen model. An 8-noded solid element, CC3DnonLinCementitious2, was utilised to model the concrete and mortar. CC3DNonLinCementitious2 element assumes a hardening regime prior to reaching the compressive strength. This material may, therefore, be used in creep calculations or when the material properties need to be changed during the analysis [19]. Longitudinal reinforcement and wire ropes were modeled using CCReinforcement elements. Two nodes were required for this element. The element CCReinforcement include involves the ability to disable the compressive response of the reinforcement. This is beneficial if this element is being utilised to imitate the behavior of reinforcement that have a very low bending stiffness, just like wire rope, so it can be assumed that when the reinforcement is loaded by compressive forces, buckling occurs and the strength of the elements in compression is negligible [19]. Loading and support plates were modeled using the 8-noded solid element CC3DelastIsotropic because it simulates linear elastic isotropic materials for 3D [31]. The concrete with stirrups was modeled using the 8-noded CCCombinedMaterial element. This element can be used to create a composite material consisting of various components, such as for instance concrete with smeared reinforcement in various directions [31]. The materials and type of elements used in the modeling are summarized in Table 2.

Al Faridi [32] conducted a convergence study and concluded that the optimal number of elements in ATENA is 1056. Since the student version of ATENA provided a maximum of only 200 elements for the 3-D analysis, the meshing had to be done thoroughly so that the number of elements made did not exceed the limit of a maximum number of meshing elements. The meshing plans for each specimen model are shown in Figure 10. The control beam model (BK) had a total of 197 elements with 192 volume elements and 5 lineal elements. The strengthened beam model 1 (BP1) had a total of 161 elements with 152 volume elements and 9 lineal elements. Meanwhile, the strengthened beam model 2 (BP2) had a total of 191 elements with 180 volume elements and 11 lineal elements.

The application of constraint conditions in the analysis consisted of a support constraint condition and a surface constraint condition. The support constraint condition was applied in the analysis to represent support in the experimental test specimens. It was applied by giving the displacement value of zero in the Y direction using constraint for line. The value was applied to a line in the middle part of the support steel plates in the model. In addition to the support line, the constraint condition was also applied using constraint for surface to the surface. This is because the simulation was done for only half of a beam. To calculate the responses occurring in the model, the load and flexural observation points for the Y direction were applied. Observations were conducted using monitor for point with displacement output to measure the deformation while compact external forces output was used to measure the load. For the displacement control method, the load used is in the form of displacement loads which is applied using displacement for point at the rate of 1 mm.

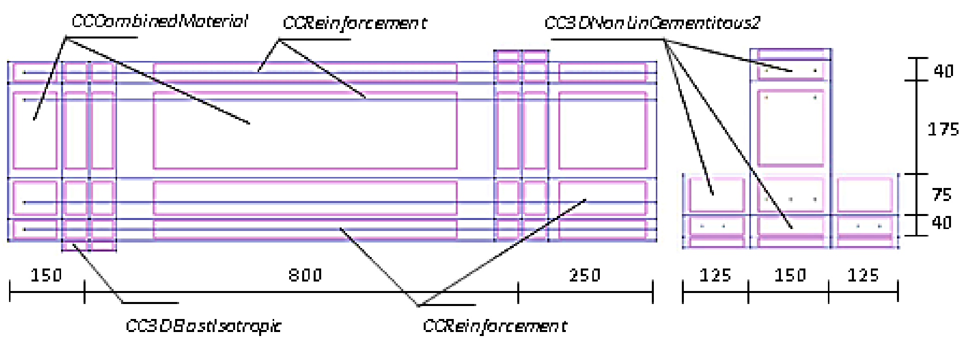

Figure 9 Model of finite element analysis for half of a section

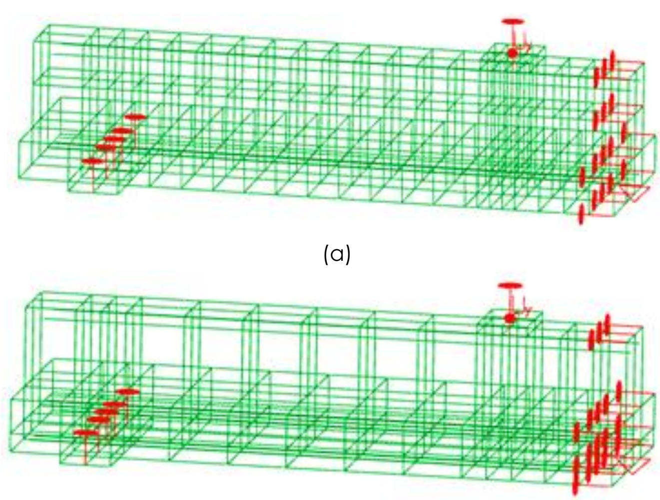

(a)

(b)

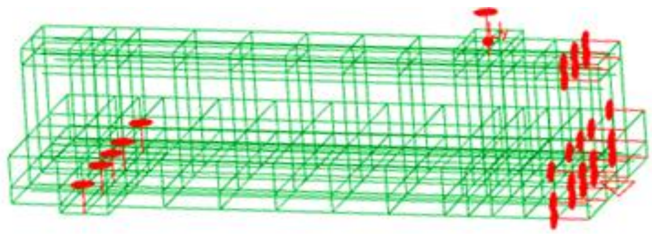

(c)

Figure 10 The meshing plans for each specimen model: (a) control beam (BK); (b) strengthened beam type 1 (BP1); (c) strengthened beam type 2 (BP2)

Table 2 Materials and types of elements

Materials	Element type	Properties	Data
Concrete	*CC3DnonLinCementitous2*	Compression strength	32.26
		Young's modulus, E_c	25756.899
Mortar	*CC3DnonLinCementitous2*	Compression strength	49.70
		Young's modulus, E_c	30305.411
Reinforcement P8	*CCReinforcement*	Young's modulus, E_s	200000
		Ultimate stress, f_u	540.63
		Yield stress, f_y	382.52
		Area of reinforcement, *A*	0.00005024
Reinforcement D13	*CCReinforcement*	Young's modulus, E_s	200000
		Ultimate stress, f_u	735.30
		Yield stress, f_y	480.65
		Area of reinforcement, *A*	0.000132665
Wire rope	*CCReinforcement*	Young's modulus, E_s	35725
		Ultimate stress, f_u	740.582
		Yield stress, f_y	-
		Area of reinforcement, *A*	0.0000785
Concrete stirrup P8-40	*CCCombinedMaterial*	Area of shear reinforcment, A_v	0.0008038
		Ratio of direction x reinforcement (1)	0.0032154
		Ratio of direction y reinforcement (2)	0.0053589
		Ratio of direction z reinforcement (3)	0
Concrete stirrup P8-100	*CCCombinedMaterial*	Area of shear reinforcment, A_v	0.0003517
		Ratio of direction x reinforcement (1)	0.0014067
		Ratio of direction y reinforcement (2)	0.0023445
		Ratio of direction z reinforcement (3)	0
Loading and support plates	*CC3DElastIsotropic*	Young's modulus, E_s	200000
		Poisson's ratio, *v*	0.3

3.0 RESULTS AND DISCUSSION

3.1 Load-Deflection Relationship

From the results of the finite element analysis conducted using ATENA, graphs of the load–displacement relationship could be created and then compared with the results of the experimental tests. The load–displacement relationship resulting from the finite element analysis behaved similarly to the results of the experimental test. The study conducted previously by Hidayat [33] proves that, in reality, a concrete member is not uniform and does not possess homogeneous strength throughout its depth. Since the material properties were homogeneous in all segments of the analysis, there were consistent slope differences between the results of the finite element analysis and those of the experimental test [24]. The graphical comparison of the load–displacement relationship for the control beam is shown in Figure 11 while the strengthened beams are shown in Figure 12.

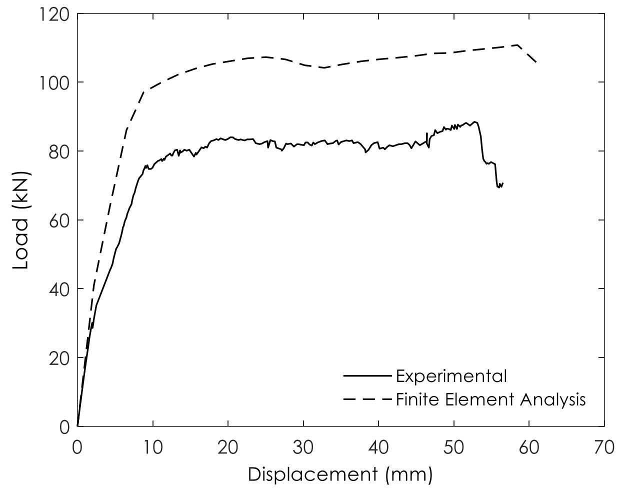

Figure 11 Load–displacement relationship of control beams (BK) [20]

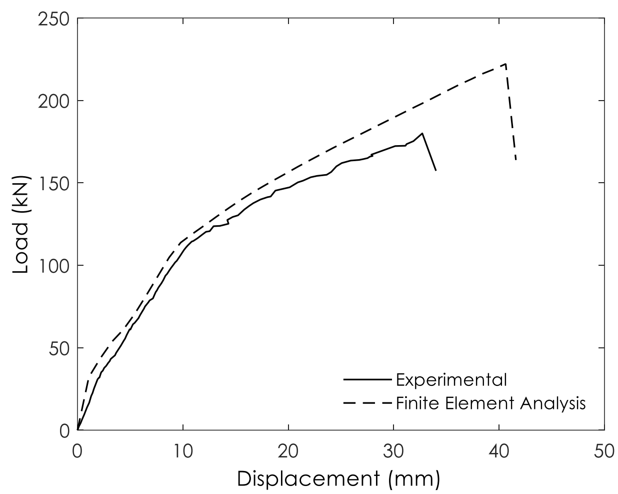

(a)

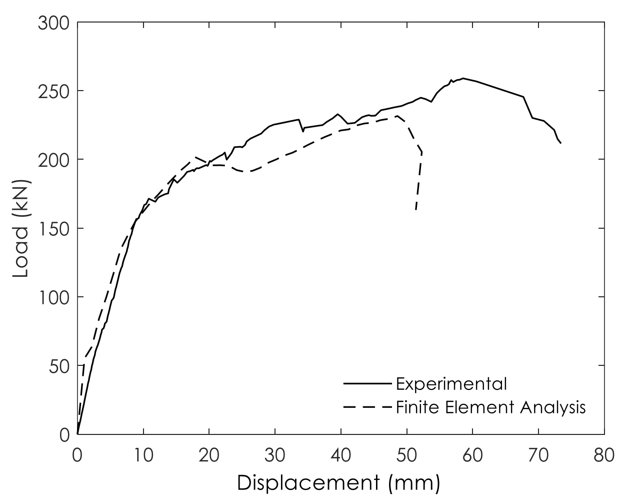

(b)

Figure 12 Load–displacement relationship of strengthened beams: (a) strengthened beam type 1 (BP1); (b) strengthened beam type 2 (BP2)

3.2 Load-Carrying Capacity

The comparison of the load-carrying capacity resulting from the finite element analysis and the experimental test is shown in Figure 13. It can be observed that the load-carrying capacity resulting from the finite element analysis was quite similiar to the experimental results, with ratios of 1.25, 1.23, and 0.89 respectively for BK, BP1 and BP2. The difference may be affected by the assumed perfect bond among materials, so the finite element analysis works well, and no slip occurred as in the experimental tests [24]. Moreover, due to the characteristics of the material, the outcomes acquired from experimental and finite element analysis are partially different. Concrete has a heterogeneous nature so that it does not show the same material characteristics under all directions. However, when defining the material characteristic, the modeling is conducted in the finite element analysis by accepting that concrete has a homogeneous mixture in all directions [34].

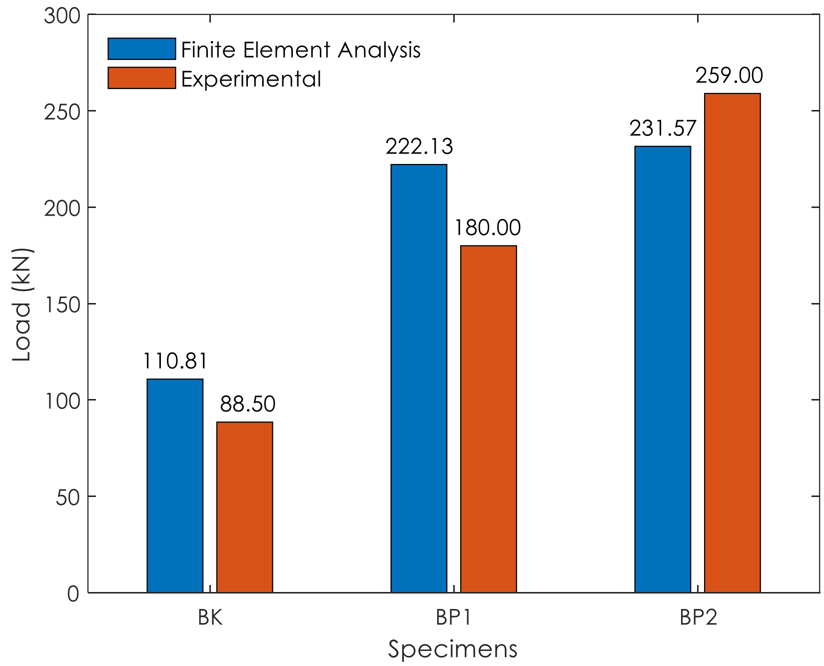

Figure 13 Load-carrying capacity

3.3 Stiffness and Ductility

The comparisons of effective stiffness and ductility resulting from the finite element analysis and experimental test can be seen in Table 3 and Table 4. Table 3 shows that the ratios of the effective stiffness based on the finite element analysis to the effective stiffness resulting from the experimental test were 1.45, 1.15, and 1.86 respectively for BK, BP1, and BP2. It was found that the behavior obtained from the finite element analysis was stiffer, with an average of 48.67%, which is relatively high in the context of this study. This is because there was no bond slip of the wire ropes than that obtained by the experimental test [24].

To determine the ductility of a structure or element structure, the ductility index, which is the ratio of ultimate deflection to yield deflection, is used. Ultimate deflection is considered as the deflection where the load has fallen to 80% of the peak load after attaining the peak. The yield deflection, on the other hand, is referred to as the deflection at the hypothetical yield point of an equivalent elasto-plastic system whereby its equivalent elastic stiffness is considered as the secant stiffness at 75% of the peak load before attaining the peak load with the yield strength being considered as the peak load. The ratios of ductility based on the finite element analysis to the ductility resulting from the experimental test were 1.11, 0.63, and 1.01 respectively for BK, BP1, and BP2.

Table 3 Comparison of effective stiffness

Codes	Results of experimental test	Results of finite element analysis	Ratio
BK	9039.84	13139.05	1.45
BP1	6297.20	7282.95	1.15
BP2	7766.89	14473.12	1.86

Table 4 Comparison of ductility

Codes	Results of experimental test	Results of finite element analysis	Ratio
BK	6.93	6.26	1.11
BP1	1.32	2.09	0.63
BP2	3.01	2.99	1.01

3.4 Cracking Patterns

It was reported previously [20] that the first crack in the control beam (BK) occurred in the area around midspan when the load reached 40.98 kN with a deflection of 2.18 mm. The maximum load of 110.81 kN was achieved with the corresponding deflection of 58.45 mm. Strengthened beam 1 (BP1) had the first crack at a load of 31.14 kN with a deflection of 1.00 mm. The maximum load of 222.13 kN was achieved with the corresponding deflection of 40.00 mm. The first crack in strengthened beam 2 (BP2) occurred when the load reached 55.18 kN with a deflection of 1.00 mm at midspan. The maximum load of 231.57 kN was achieved with the corresponding deflection of 48 mm. The crack propagation created from the finite element analysis revealed a flexural failure on all models. Figure 14 shows the cracking patterns.

It was discovered that the findings obtained from ATENA finite element program are significantly linked with the experiment's results. This demonstrates that ATENA modeling provides us consistent results similar to previous studies. In addition, the resulting models can be beneficial to reduce both costing and time. Furthermore, all mistakes can be prevented.

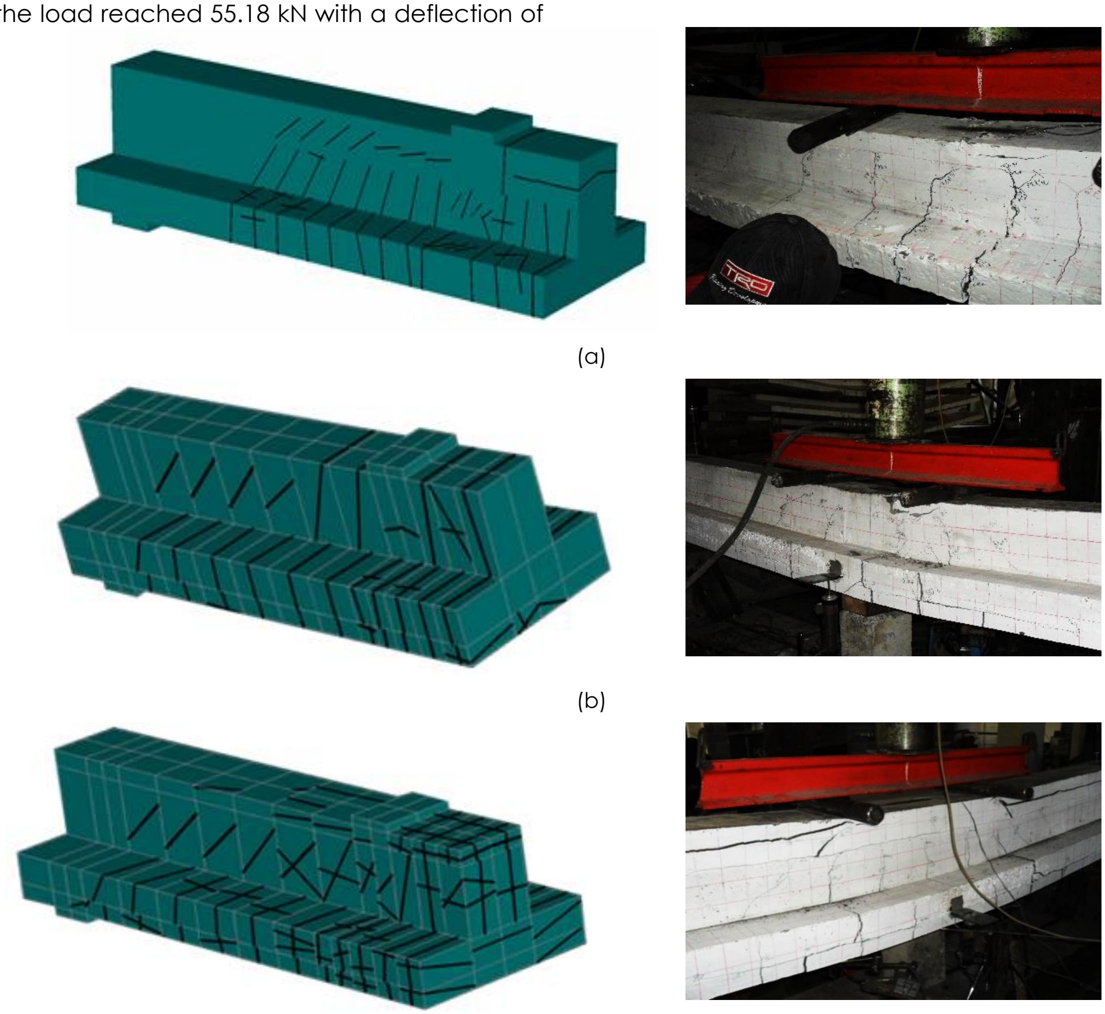

(a)

(b)

(c)

Figure 14 The cracking patterns: (a) control beam (BK); (b) strengthened beam type 1 (BP1);(c) strengthened beam type 2 (BP2)

4.0 CONCLUSION

To conclude, the load–displacement relationship resulting from the finite element analysis behaves similarly to those of the experimental results. The ratios of the load-carrying capacity resulting from the finite element analysis to those of the experimental results were 1.25, 1.23, and 0.89 respectively for BK, BP1 and BP2, while the ratios of the effective stiffness resulting from the finite element analysis to the effective stiffness resulting from the experimental test were respectively by 1.45, 1.15, and 1.86 for BK, BP1, and BP2. The ratios of ductility resulting from the finite element analysis to the effective stiffness resulting from the experimental test were respectively 1.11, 0.63, and 1.01 for BK, BP1, and BP2. The crack propagation showed that the flexural failure occurred in all models. The finite element analysis conducted in this paper used only the parameters identical to those in the experimental test results. Therefore, the different strength and modulus of elasticity of the materials should be analyzed for merit further study. Various types of elements, a higher number of meshing elements, and bond-slip behavior are candidates for future work.

Acknowledgements

The authors express their gratitude and appreciation to the Research and Public Services Institution (LPPM) of Jenderal Soedirman University for funding this study, and to Bidono and all the member of the Computer Aided Strctural Analysis Laboratory, Department of Civil Engineering, National Cheng Kung University for providing assistance so that this study accomplished its goals. The authors also thank the anonymous reviewers, whose comments greatly improved the paper.

References

[1] Park, T. W. 2012. Inspection of Collapse Cause of Sampoong Department Store. *Forensic Science International*. 217(1-3): 119-126.

[2] Haryanto, Y., Sudibyo, G. H. and Effendi, F. C. A. 2017. Preliminary Seismic Hazard Assessment of the Oral and Dental Hospital of Jenderal Soedirman University Indonesia. *Procedia Engineering*. 171: 1025-1034.

[3] Haryanto, Y., Gan, B. S., Wariyatno, N. G., and Indriyati, E. W. 2017. The Performance of a Ten-story Irregular Apartment Building Model under Seismic Load in Purbalingga Regency Indonesia. *ARPN Journal of Engineering and Applied Sciences.* 12(17): 4858-4866.

[4] Haryanto, Y., Gan, B. S., Wariyatno, N. G., and Indriyati, E. W. 2018. Seismic Performance of a High-rise Residential Building Model in Purwokerto, Indonesia. *MATEC Web of Conferences*. 192: 02002.

[5] Widyaningrum, A., Haryanto, Y., and Hermanto, N. I. S. 2018. A Structural Performance Evaluation of Vertical Housing Model Due to the Increased Seismic Loads in Semarang, Indonesia Using a Pushover Analysis. *MATEC Web of Conferences.* 195: 02018.

[6] Raoof, M. and Davies, T. J. 2003. Simple Determination of the Axial Stiffness for Large Diameter Independent Wire Rope Core or Fibre. *The Journal of Strain Analysis for Engineering Design*. 38(6): 577-586.

[7] Avak, R. and Willie, F. 2005. Experimental Investigations and Modeling of Bond between Round Strand Ropes and Concrete. *The 11th International Conference on Fracture (ICF)*. Turin, Italy.

[8] Kim, S. Y., Yang, K. H., Byun, H. Y. and Ashour, A. F. 2007. Tests of Reinforced Concrete Beams Strengthened with Wire Rope Units. *Engineering Structures*. 29: 2711-2722.

[9] Yang, K. H., Byun, H. Y. and Ashour, A. F. 2009. Shear Strengthening of Continuous Reinforced Concrete T-Beams Using Wire Rope Units. *Engineering Structures*. 31: 1154-1165.

[10] Haryanto, Y. 2011. Efektifitas Wire Rope Sebagai Perkuatan Pada Daerah Momen Negatif Balok Beton Bertulang Tampang T. *Dinamika Rekayasa*. 7(2): 36-42.

[11] Atmajayanti, A. T., Satyarno, I. and Saputra, A. 2013. Pengaruh Penggunaan Wire Rope sebagai Perkuatan Lentur Terhadap Kekuatan dan Daktilitas Balok Beton Bertulang Tampang T. *Konferensi Nasional Teknik Sipil 7*, Surakarta, Indonesia.

[12] Haryanto, Y., Wariyatno, N. G. and Sudibyo, G H. 2013. Pengaruh Gaya Prategang Awal Terhadap Efektifitas Wire Rope sebagai Perkuatan Daerah Momen Negatif Balok Beton Bertulang Tampang T. *Seminar Nasional Teknik Sipil IX*. Surabaya, Indonesia.

[13] Galuh, D. L. C. 2015. The Effectiveness of the Use of Wire Rope Flexural as the Negative Moment Reinforcement in T-Sectional Reinforced Concrete Beam. *International Conference on Quality in Research*, Lombok, Indonesia.

[14] Galuh, D. L. C. 2018. Comparative Analysis Layes Method of T-Beam Reinforcement. *IOP Conf. Series: Materials Science and Engineering*. 316: 012043.

[15] Yanuar, Y., Gan, B. S., Widyaningrum, A., Wariyatno, N. G. and Fadli, A. 2018. On the Performance of Steel Wire Rope As the External Strengthening of RC Beams with Different End-Anchor Type. *Jurnal Teknologi (Sciences and Engineering)*. 80(5): 145-154.

[16] Han, A., Gan, B. S. and Pratama, M. M A. 2016. Effects of Graded Concrete on Compressive Strengths. *International Journal of Technology*. 7(5): 732-740.

[17] Hu, H.-T., Lin, F.-M. and Jan, Y.-Y. 2004. Nonlinear finite Element Analysis of Reinforced Concrete Beams Strengthened by Fber-reinforced Plastics. *Composite Structures*. 63: 271-281.

[18] Lesmana, C. and Hu, H.-T. 2015. Nonlinear Finite Element Analysis of Rectangular Reinforced Concrete Slabs Strengthened by Fiber Reinforced Plastics. *Scientia Iranica A*. 22(3): 615-628.

[19] Cervenka, V., Jendele, L. and Cervenka, J. 2018. *ATENA Program Documentation Part 1; Theory*. Prague, Czech Republic: Cervenka Consulting.

[20] Pangestuti, E. K. and Effendi, M. K. 2010. Perilaku Lentur Balok-L Beton Bertulang Berlubang Ditinjau Secara Eksperimental dan Analisis Numerik Memakai Software GID-ATENA. *Jurnal Teknik Sipil dan Perencanaan*. 12(2): 121-130.

[21] Sukarno, P., Muslikh and Sulsityo, D. 2011. Analisis Lentur Balok Penampang T Berlubang Memanjang Menggunakan Metode Elemen Hingga Non-linier. *Jurnal Ilmiah Semesta Teknika*. 14(1): 1-14.

[22] Setyawan, A. 2012. Non-linier Analisis of Stress and Prestressed Concrete Bridge Structure Deformation within the Construction Phase Using the Balanced Cantilever Method. *Jurnal Teknik Sipil Universitas Surakarta*. 13(2): 33-39.

[23] Jati, D. G. 2013. Analisis Lentur Pelat Satu Arah Beton Bertulang Berongga Bola Menggunakan Metode Elemen Hingga Non Linier. *Konferensi Nasional Teknik Sipil 7*, Surakarta, Indonesia.

[24] Haryanto, Y., Gan, B. S. and Maryoto, A. 2017. Wire Rope Flexural Bonded Strengthening System on RC-Beams: A

Finite Element Simulation. *International Journal of Technology*. 8(1): 134-144.

[25] Haryanto, Y., Gan, B. S., Widyaningrum, A. and Maryoto, A. 2017. Near Surface Bamboo Reinforcement for Flexural Strengthening of Reinforced Concrete Beams. *Jurnal Teknologi (Sciences and Engineering)*. 79(6): 233-240.

[26] Jirawattanasomkul, T., Kongwang, N., Jongvivatsakul, P. and Likitlersuang, S. 2018. Finite Element Modelling of flexural Behaviour of Geosynthetic Cementitious Composite Mat (GCCM). *Composites Part B.* 154: 33-42.

[27] Kupfer, H., Hilsdorf, H. K. and Rüsch, H. 1969. Behavior of Concrete under Biaxial Stress. *Journal ACI*. 66(8): 656-666.

[28] Hordijk, D. A. *1991. Local Approach to Fatigue of Concrete.* Doctor Dissertation, The Netherlands: Delft University of Technology.

[29] Van Mier, J. G. M. 1984. Multi-axial Strain-softening of Concrete, Part I: Fracture. *Materials and Structures.* 19(3): 179-190.

[30] Lee, W. K. 1991. An Insight into Wire Rope Geometry. *International Journal of Solids and Structures*. 28(4): 471-490.

[31] Cervenka, V., Cervenka, J., Janda, Z. and Pryl, D. 2017. *ATENA Program Documentation Part 8; User's Manual for ATENA-GiD Interface*. Prague, Czech Republic: Cervenka Consulting.

[32] Al Faridi, S. 2010. *Analisis Non-linier Elemen Hingga Struktur Balok Beton Prategang Dua Bentangan*. Mater Thesis. Yogyakarta, Indonesia: Gadjah Mada University.

[33] Hidayat, A., Purwanto, Puspowadojo, J. and Aziz, F.A. *2015.* The Influence of Graded Concrete Strength on Concrete Element. *Procedia Engineering*. 125: 1023-1029.

[34] Büyükkaragöz, A. 2010. Finite Element Analysis of the Beam Strengthened with Prefabricated Reinforced Concrete Plate. *Scientific Research and Essays*. 5(6): 533-544.